

Obtaining $\text{Si-Si}_{1-x}\text{Ge}_x-(\text{Si}_{1-x}\text{Ge}_x)_{1-z}(\text{Al}_{1-y}\text{Ga}_y\text{As})_z$ $-\text{Si}_{1-x}\text{Ge}_x-(\text{Si}_{1-x}\text{Ge}_x)_{1-z}(\text{Al}_{1-y}\text{Ga}_y\text{As})_z$ Structures from a Tin Solution-Melt in a Single Technological Cycle

A.S. SAIDOV^a, A.SH. RAZZOKOV^{b,*},
 S.I. PETRUSHENKO^c AND S.V. DUKAROV^c

^aPhysical-Technical Institute NPO "Physics-Sun" of the Academy of Sciences
 of the Republic of Uzbekistan, Ch. Aitmatova 2B, 100084, Tashkent, Uzbekistan

^bUrgench State University, Urgench, Kh. Alimjan 14, 220100, Uzbekistan

^cV.N. Karazin Kharkiv National University, Svobody square 4, 61077, Kharkiv, Ukraine

Received: 10.04.2022 & Accepted: 30.05.2022

Doi: [10.12693/APhysPolA.142.280](https://doi.org/10.12693/APhysPolA.142.280)

*e-mail: a.razzokov777@gmail.com

From a limited tin solution-melt in the temperature range of 950–700°C, $\text{Si-Si}_{1-x}\text{Ge}_x-(\text{Si}_{1-x}\text{Ge}_x)_{1-z}(\text{Al}_{1-y}\text{Ga}_y\text{As})_z$ structures on Si (111) substrates were grown by liquid-phase epitaxy in a single technological cycle. Using a scanning electron microscope, the layered composition of the grown films was determined. X-ray diffraction studies of the structure showed the dependence of the crystalline perfection of the film on the technological growth regime. The optimum mode of forced cooling rate (1 deg/minute) was established during cultivation. Some electrophysical and photoelectric properties of $\text{Si-Si}_{1-x}\text{Ge}_x-(\text{Si}_{1-x}\text{Ge}_x)_{1-z}(\text{Al}_{1-y}\text{Ga}_y\text{As})_z$ structures were determined.

topics: solution-melt, epitaxy, films, solid solution

1. Introduction

Obtaining structurally perfect $\text{Si-Al}_{1-y}\text{Ga}_y\text{As}$ heterostructures based on semiconductor materials Si (substrate) and $\text{Al}_{1-y}\text{Ga}_y\text{As}$ (film) with specific electrophysical and photoelectric properties is a very urgent task from the point of view of the prospects for their use in the field of optoelectronics. In particular, promising photodetectors, photoconverters, and cascade structures can be fabricated on their basis [1, 2].

However, the mismatch between the lattice parameters of Si and $\text{Al}_{1-y}\text{Ga}_y\text{As}$ limits the possibility of growing $\text{Al}_{1-y}\text{Ga}_y\text{As}$ epitaxial films with sufficiently low dislocation densities in the heterointerface and along the growth direction [3–5].

Methods for growing various semiconductor solid solutions on a relatively cheap Si substrate (with good thermal conductivity and lower specific gravity) and obtaining heterostructures with desired photoelectric properties have been studied by many authors [6–10]. Various technological methods were used, including the growth of epitaxial layers with different thicknesses (from nm to μm) by liquid-phase epitaxy. In [6], the combined use of liquid-phase and molecular-beam epitaxy was tested to obtain $\text{Al}_{1-y}\text{Ga}_y\text{As}$ on a Si substrate. The authors of [7] showed that samples grown by

liquid-phase epitaxy with a double junction based on a lower silicon layer are promising for solar energy. In article [11], by chemical vapor deposition of organometallic compounds with a $\text{Si}_{1-x}\text{Ge}_x$ transition layer on a Si substrate, a GaAs film with dislocation densities $N_d \simeq 8 \times 10^5 \text{ cm}^{-2}$ was obtained. The minority carrier lifetime was 10 ns. The observed time is the result of eliminating antiphase domains and maintaining the density of threading dislocations.

Some authors have used electron cyclotron resonance chemical vapor deposition (ECR-CVD) to grow thin epilayer Ge (100 nm) on Si. Then, GaAs epitaxial layers are grown on Ge/Si using metal-organic chemical vapor deposition (MOCVD) [12].

In this work, in a single technological cycle, $\text{Si-Si}_{1-x}\text{Ge}_x-(\text{Si}_{1-x}\text{Ge}_x)_{1-z}(\text{Al}_{1-y}\text{Ga}_y\text{As})_z$ structure with buffer layer $\text{Si}_{1-x}\text{Ge}_x$ was grown on the Si substrate using simpler technological approaches.

The solid solution $\text{Si}_{1-x}\text{Ge}_x$, $(\text{Si}_{1-x}\text{Ge}_x)_{1-z}(\text{Al}_{1-y}\text{Ga}_y\text{As})_z$ allows one to vary the main electrical parameters of the semiconductor material and structures based on them within certain limits with a change in their chemical composition. It becomes possible to choose materials with specific characteristics when creating specific

semiconductor devices. The growth of $\text{Si}_{1-x}\text{Ge}_x$, $(\text{Si}_{1-x}\text{Ge}_x)_{1-z}(\text{Al}_{1-y}\text{Ga}_y\text{As})_z$ epitaxial layers on Si substrates reduces to a minimum the stresses arising due to the mismatch between the crystal lattices of the substrates and the layers being grown, which causes the crystalline perfection of films and structures based on them.

Thus, the prospects of using liquid-phase epitaxy to obtain $\text{Si-Si}_{1-x}\text{Ge}_x-(\text{Si}_{1-x}\text{Ge}_x)_{1-z}(\text{Al}_{1-y}\text{Ga}_y\text{As})_z-\text{Si}_{1-x}\text{Ge}_x-(\text{Si}_{1-x}\text{Ge}_x)_{1-z}(\text{Al}_{1-y}\text{Ga}_y\text{As})_z$ heterostructures on the surface of single-crystal silicon substrates in a single growth cycle, are the reduction of energy costs, the time of the technological process and the number of chemical components used.

2. Methodology of the experiment

Using the method of liquid-phase epitaxy, we obtained in the temperature range of 950–700°C from a tin solution-melt in a single technological cycle the heterostructure $\text{Si-Si}_{1-x}\text{Ge}_x-(\text{Si}_{1-x}\text{Ge}_x)_{1-z}(\text{Al}_{1-y}\text{Ga}_y\text{As})_z-\text{Si}_{1-x}\text{Ge}_x-(\text{Si}_{1-x}\text{Ge}_x)_{1-z}(\text{Al}_{1-y}\text{Ga}_y\text{As})_z$.

As substrates, plates of a Si single crystal with a diameter of 40 mm and a thickness of 400 μm , oriented along the (111) direction, and having p-type conductivity with specific resistances $\rho \approx 0.5 \Omega \text{ cm}$ and concentration $n = 3 \times 10^{17} \text{ s/m}^3$, were used.

For growing heterostructures $\text{Si-Si}_{1-x}\text{Ge}_x-(\text{Si}_{1-x}\text{Ge}_x)_{1-z}(\text{Al}_{1-y}\text{Ga}_y\text{As})_z-\text{Si}_{1-x}\text{Ge}_x-(\text{Si}_{1-x}\text{Ge}_x)_{1-z}(\text{Al}_{1-y}\text{Ga}_y\text{As})_z$, we used a vertical type quartz reactor with horizontal substrates in an EPOS facility. The growth of the epitaxial layer was carried out from a small volume of a tin solution-melt limited by two substrates in an atmosphere of hydrogen purified by palladium, which made it possible to minimize the amount of the spent solution-melt. First, a vacuum was created in the reactor to a residual pressure of 10^{-2} Pa , then purified hydrogen was passed through the reactor for 20 min, and then the heating process began. When the temperature reached the required value, the system switched to an automatic mode. The solution-melt was homogenized for 40–60 min. Then, the substrates on the graphite holder were brought into contact with the solution-melt, and after filling the gaps between the substrates with the solution-melt, they were raised by 1 cm above the level of the solution. The growth of epitaxial layers $\text{Si}_{1-x}\text{Ge}_x$ was stopped at the right time by draining the solution-melt from the substrates using a centrifuge. The composition of the melt solution consisting of Si, Ge, Al, Ga, As, and Sn was determined from the phase diagram of the Sn–Si, Sn–Ge, Sn–Al, and Sn–GaAs binary alloy [13–15].

In the growing process, respectively, the chemical composition and structure, thickness, and variability of the solid solution are controlled as follows. First, the compositions of the components and

the solvent are selected, taking into account the state diagram of the solubility of the components at a certain temperature, which is the temperature of the beginning of crystallization. Depending on the crystallization onset temperature, we can choose the composition of the melt solution and, accordingly, the initial chemical composition of the epitaxial layer in contact with the film substrate. At the next stage, by choosing the temperature of the end of crystallization, we can control the film thickness, i.e., establish the composition of the components on the surface of the film, by stopping its growth at a certain stage.

Also, a smooth change in the composition of the film (varizon) along the direction of growth is controlled with a gap between horizontally located substrates, and the volume between them is filled with a solution-melt. Forced program cooling at the beginning of the growth of epitaxial layers makes it possible to control the film growth rate (which is one of the main determinants of film quality).

The process of growing epitaxial layers and structures based on them is limited in terms of capabilities, but it gives a significant advantage for the growth of a solid solution with variable compositions. Thus, based on technological capabilities, the chemical composition of the solid solution is controlled.

Heterostructural samples were grown in a single technological cycle from a limited tin solution-melt at a temperature range from $T_{OC} = 950^\circ\text{C}$ (crystallization onset temperature) to $T_{EC} = 700^\circ\text{C}$ (crystallization termination temperature). The rate of forced cooling during growth was 1 deg/min.

To obtain $\text{Si-Si}_{1-x}\text{Ge}_x-(\text{Si}_{1-x}\text{Ge}_x)_{1-z}(\text{Al}_{1-y}\text{Ga}_y\text{As})_z-\text{Si}_{1-x}\text{Ge}_x-(\text{Si}_{1-x}\text{Ge}_x)_{1-z}(\text{Al}_{1-y}\text{Ga}_y\text{As})_z$ the intermediate $\text{Si}_{1-x}\text{Ge}_x$ epitaxial layer served as a buffer. The intermediate layers reduce the mismatch between the lattice parameters of the Si substrate ($a_{\text{Si}} = 5.431 \text{ \AA}$) and the AlGaAs film ($a_{\text{AlGaAs}} = 5.654 \text{ \AA}$, $a_{\text{Ge}} = 5,658 \text{ \AA}$) due to smoothing.

The grown epitaxial layers and heterostructures were studied using a Tescan Vega 3 LMH scanning electron microscope equipped with a Bruker XFlash 5010 characteristic X-ray detector. An example and a sketch (model) of elemental maps obtained on a transverse cleavage of a sample are shown in Fig. 1a and b.

3. Results and discussion

In this work, a general quantitative analysis of the composition from the side of the end (from the substrate to the film surface along the direction of growth in a stepwise mode) of $\text{Si-Si}_{1-x}\text{Ge}_x-(\text{Si}_{1-x}\text{Ge}_x)_{1-z}(\text{Al}_{1-y}\text{Ga}_y\text{As})_z-\text{Si}_{1-x}\text{Ge}_x-(\text{Si}_{1-x}\text{Ge}_x)_{1-z}(\text{Al}_{1-y}\text{Ga}_y\text{As})_z$ is performed. Examples of EDS spectra obtained from different cleavage areas are shown in Fig. 2a and b.

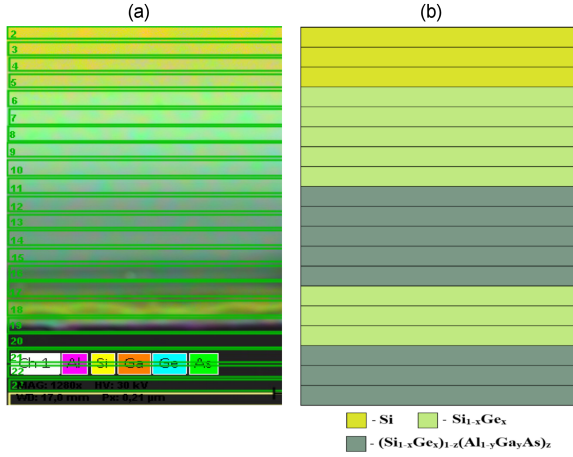


Fig. 1. (a) Elemental maps obtained from the cleavage of structures $\text{Si-Si}_{1-x}\text{Ge}_x-(\text{Si}_{1-x}\text{Ge}_x)_{1-z}(\text{Al}_{1-y}\text{Ga}_y\text{As})_z-\text{Si}_{1-x}\text{Ge}_x-(\text{Si}_{1-x}\text{Ge}_x)_{1-z}(\text{Al}_{1-y}\text{Ga}_y\text{As})_z$. The length of the horizontal side is $55 \mu\text{m}$. (b) Sketch of the elemental map obtained from the cleavage of structures $\text{Si-Si}_{1-x}\text{Ge}_x-(\text{Si}_{1-x}\text{Ge}_x)_{1-z}(\text{Al}_{1-y}\text{Ga}_y\text{As})_z-\text{Si}_{1-x}\text{Ge}_x-(\text{Si}_{1-x}\text{Ge}_x)_{1-z}(\text{Al}_{1-y}\text{Ga}_y\text{As})_z$.

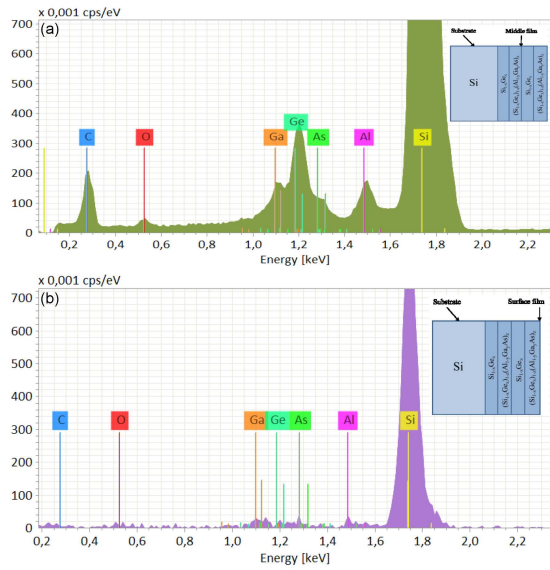


Fig. 2. (a) An example of the EDS spectrum of a cleavage of the structure $\text{Si-Si}_{1-x}\text{Ge}_x-(\text{Si}_{1-x}\text{Ge}_x)_{1-z}(\text{Al}_{1-y}\text{Ga}_y\text{As})_z-\text{Si}_{1-x}\text{Ge}_x-(\text{Si}_{1-x}\text{Ge}_x)_{1-z}(\text{Al}_{1-y}\text{Ga}_y\text{As})_z$. (b) An example of an EDS spectrum obtained from the side of the substrate to the film surface along the direction of growth) of structures $\text{Si-Si}_{1-x}\text{Ge}_x-(\text{Si}_{1-x}\text{Ge}_x)_{1-z}(\text{Al}_{1-y}\text{Ga}_y\text{As})_z-\text{Si}_{1-x}\text{Ge}_x-(\text{Si}_{1-x}\text{Ge}_x)_{1-z}(\text{Al}_{1-y}\text{Ga}_y\text{As})_z$.

The quantitative composition of the middle (Fig. 2a) and surface (Fig. 2b) of the cleavage of the grown structures shows changes along the direction of film growth with alternating layers.

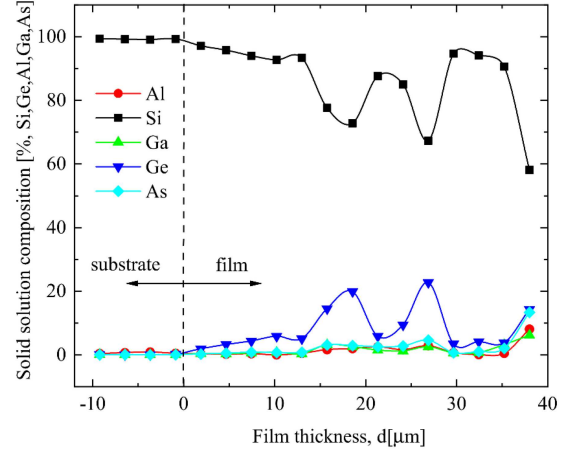


Fig. 3. Distribution of components over the thickness of the epitaxial layers of the structure $\text{Si-Si}_{1-x}\text{Ge}_x-(\text{Si}_{1-x}\text{Ge}_x)_{1-z}(\text{Al}_{1-y}\text{Ga}_y\text{As})_z-\text{Si}_{1-x}\text{Ge}_x-(\text{Si}_{1-x}\text{Ge}_x)_{1-z}(\text{Al}_{1-y}\text{Ga}_y\text{As})_z$. (When quantifying the EDS spectrum for all impurity elements, mainly sorbed from the atmosphere, the “only deconvolution” mode was chosen).

The results showed that on a silicon substrate with $\langle 111 \rangle$ orientation there is a layer of $\text{Si}_{1-x}\text{Ge}_x$ with a thickness of $12-14 \mu\text{m}$. This layer is deposited from a saturated solution-melt of Si-Ge-Al-Ga-As-Sn , due to its limited volume. This makes it possible to obtain graded-gap epitaxial layers with a variable chemical composition along the film growth direction. At the next stage of growth, Al-Ga-As components are next deposited, with which the solution-melt is saturated at a given temperature. It should be noted that the orientation of the single-crystal substrate in the $\langle 111 \rangle$ direction is the most favorable for the described growth process.

At the next stage, the concentration of germanium and silicon in the solution-melt increases. Due to this, the $\text{Si}_{1-x}\text{Ge}_x$ buffer layer grows again. The next $\text{Al}_{1-y}\text{Ga}_y\text{As}$ epilayer continues the existing crystallographic orientation of the previously formed structures. Its growth continues after the solution-melt is depleted of silicon and germanium (Fig. 3). Due to the successive alternation of these processes, which occurs naturally, it was possible to obtain a four-layer $\text{Si-Si}_{1-x}\text{Ge}_x-(\text{Si}_{1-x}\text{Ge}_x)_{1-z}(\text{Al}_{1-y}\text{Ga}_y\text{As})_z-\text{Si}_{1-x}\text{Ge}_x-(\text{Si}_{1-x}\text{Ge}_x)_{1-z}(\text{Al}_{1-y}\text{Ga}_y\text{As})_z$ heterostructure.

Thus, the possibility of obtaining $\text{Si-Si}_{1-x}\text{Ge}_x-(\text{Si}_{1-x}\text{Ge}_x)_{1-z}(\text{Al}_{1-y}\text{Ga}_y\text{As})_z-\text{Si}_{1-x}\text{Ge}_x-(\text{Si}_{1-x}\text{Ge}_x)_{1-z}(\text{Al}_{1-y}\text{Ga}_y\text{As})_z$ structures from a melt solution in a single technological growth process is shown.

X-ray diffraction studies were performed using a D2 Phaser-Bruker X-ray diffractometer. The survey was carried out in the Bragg-Brentano geometry. $\text{Cu } K_\alpha$ radiation and β rotation of the sample

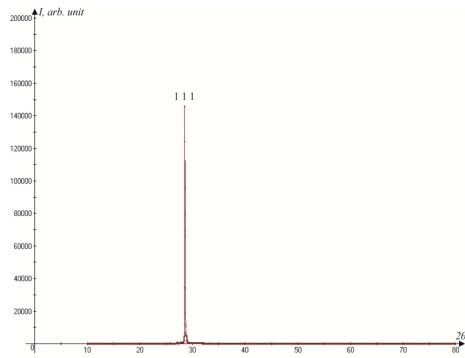


Fig. 4. X-ray diffraction pattern obtained from a sample of $\text{Si-Si}_{1-x}\text{Ge}_x-(\text{Si}_{1-x}\text{Ge}_x)_{1-z}(\text{Al}_{1-y}\text{Ga}_y\text{As})_z-\text{Si}_{1-x}\text{Ge}_x-(\text{Si}_{1-x}\text{Ge}_x)_{1-z}(\text{Al}_{1-y}\text{Ga}_y\text{As})_z$ structures grown with speed of 1 deg/minute forced cooling.

were used. An example of the obtained X-ray pattern is shown in Fig. 4. The inset presents an enlarged segment showing low-intensity peaks.

A feature of the obtained X-ray patterns is the extremely high intensity of the main peak, against which the rest of the reflections present in the X-ray patterns are lost. This type of X-ray diffraction pattern is typical for single crystals, but it is difficult to analyze.

The interplanar spacing corresponding to the most intense peak is close to the interplanar spacing of silicon (111). This, along with the absence of reflections that could be attributed to other crystallographic planes, indicates the single-crystal nature of the sample. Small differences between the observed interplanar spacing and the expected one are probably associated with the formation of solid solutions.

A sample of $\text{Si-Si}_{1-x}\text{Ge}_x-(\text{Si}_{1-x}\text{Ge}_x)_{1-z}(\text{Al}_{1-y}\text{Ga}_y\text{As})_z-\text{Si}_{1-x}\text{Ge}_x-(\text{Si}_{1-x}\text{Ge}_x)_{1-z}(\text{Al}_{1-y}\text{Ga}_y\text{As})_z$ grown at a rate of 1 deg/minute forced cooling is the most perfect crystallographically. It is characterized by the minimum half-width of diffraction lines and the smallest number of spurious reflections (Fig. 4).

The sample grown at a rate of 1.7 deg/min by forced cooling looks the least perfect (Fig. 5). In addition to the presence of many sidelines, the half-width of the main peak slightly increases. On its diffraction patterns, in addition to the peak from a single crystal of silicon, reflections are observed that can be compared with a solid solution of germanium and aluminum gallium arsenide.

In this case, the observed peaks of the solid solution (111), (220), and (311) belong to different families of crystallographic planes. This indicates the polycrystalline nature of the layer formed on the surface of this sample. Also, hard-to-identify peaks are observed on the X-ray patterns, indicating the low quality of the coating obtained under these technological conditions.

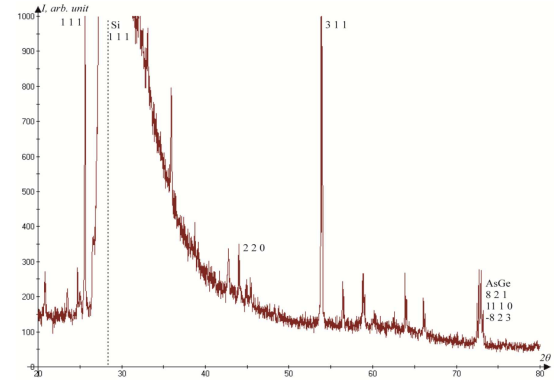


Fig. 5. X-ray diffraction pattern obtained from a sample of $\text{Si-Si}_{1-x}\text{Ge}_x-(\text{Si}_{1-x}\text{Ge}_x)_{1-z}(\text{Al}_{1-y}\text{Ga}_y\text{As})_z-\text{Si}_{1-x}\text{Ge}_x-(\text{Si}_{1-x}\text{Ge}_x)_{1-z}(\text{Al}_{1-y}\text{Ga}_y\text{As})_z$ structures grown with speed 1.7 deg/min forced cooling. The unsigned diffraction pattern shows the Miller indices, which were assigned to the Si-GaAs solid solution.

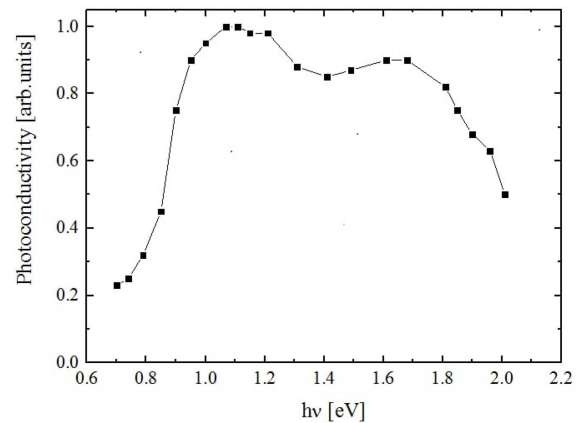


Fig. 6. Photosensitivity of the structure $\text{pSi-Si}_{1-x}\text{Ge}_x-\text{n}(\text{Si}_{1-x}\text{Ge}_x)_{1-z}(\text{Al}_{1-y}\text{Ga}_y\text{As})_z-\text{nSi}_{1-x}\text{Ge}_x-\text{n}(\text{Si}_{1-x}\text{Ge}_x)_{1-z}(\text{Al}_{1-y}\text{Ga}_y\text{As})_z$ in the photodiode mode at a temperature of 300 K.

Electrophysical and photoelectric studies of heterostructures $\text{Si-Si}_{1-x}\text{Ge}_x-(\text{Si}_{1-x}\text{Ge}_x)_{1-z}(\text{Al}_{1-y}\text{Ga}_y\text{As})_z-\text{Si}_{1-x}\text{Ge}_x-(\text{Si}_{1-x}\text{Ge}_x)_{1-z}(\text{Al}_{1-y}\text{Ga}_y\text{As})_z$ showed their promise for solving applied tasks. The films had n-type conductivity, with resistivity $\rho = 0.5-12 \Omega \text{ cm}$. Using Hall measurements, the mobility (μ) and charge carrier concentration (n) of the film were determined as $\mu_n = 500-1100 \text{ cm}^2/(\text{V s})$, $n = 5 \times 10^{17}-2 \times 10^{18} \text{ cm}^{-3}$ (at a temperature of 300 K).

The dependence of the photosensitivity of heterostructures $\text{pSi-nSi}_{1-x}\text{Ge}_x-\text{n}(\text{Si}_{1-x}\text{Ge}_x)_{1-z}(\text{Al}_{1-y}\text{Ga}_y\text{As})_z-\text{nSi}_{1-x}\text{Ge}_x-\text{n}(\text{Si}_{1-x}\text{Ge}_x)_{1-z}(\text{Al}_{1-y}\text{Ga}_y\text{As})_z$ on the energy of incident quanta was obtained in photodiode mode. The contacts were made from the side of the substrate and the film. Illumination was carried

out from the side of the films. Figure 6 shows that the spectral dependence of the photosensitivity $\text{pSi-nSi}_{1-x}\text{Ge}_x\text{-n(Si}_{1-x}\text{Ge}_x)_{1-z}(\text{Al}_{1-y}\text{Ga}_y\text{As})_z\text{-nSi}_{1-x}\text{Ge}_x\text{-n(Si}_{1-x}\text{Ge}_x)_{1-z}(\text{Al}_{1-y}\text{Ga}_y\text{As})_z$ heterostructures has a wide spectral band in the range from 0.72 to 1.9 eV.

This is due to a smooth change in the film composition along the growth direction. Along with the change in the composition of the epitaxial layers, the optical properties of the film also change smoothly. The photosensitivity in the short-wavelength region is explained by the relatively weak absorption of this radiation by the solid solution. Short-wavelength quanta are partially absorbed in the upper $\text{Al}_{1-y}\text{Ga}_y\text{As}$ layers, and those that have not had time to be absorbed in the upper layers of the solid solution with a narrow band gap penetrate into the film and are absorbed in the $\text{Si}_{1-x}\text{Ge}_x$ layers.

4. Conclusion

The paper shows the possibility of obtaining $\text{Al}_{1-y}\text{Ga}_y\text{As}$ epitaxial layers and structures $\text{Si-Si}_{1-x}\text{Ge}_x\text{-n(Si}_{1-x}\text{Ge}_x)_{1-z}(\text{Al}_{1-y}\text{Ga}_y\text{As})_z\text{-Si}_{1-x}\text{Ge}_x\text{-n(Si}_{1-x}\text{Ge}_x)_{1-z}(\text{Al}_{1-y}\text{Ga}_y\text{As})_z$ using the method of liquid epitaxy $(\text{Al}_{1-y}\text{Ga}_y\text{As})_z$ on a substrate (relatively cheap compared to other semiconductor materials) $\text{Si} \langle 111 \rangle$ from a tin solution-melt. Using $\text{Si}_{1-x}\text{Ge}_x$ epitaxial layers as a buffer layer between Si substrates and $\text{Al}_{1-y}\text{Ga}_y\text{As}$ films (that is, by smoothing out the difference in the lattice parameters of the substrate-film) and taking into account the saturation of the chemical composition of the Sn-Si-Ge-Ga-As melt solution at a certain interval temperature (950–700°C) for the first time in a single technological cycle, structures $\text{pSi-Si}_{1-x}\text{Ge}_x\text{-n(Si}_{1-x}\text{Ge}_x)_{1-z}(\text{Al}_{1-y}\text{Ga}_y\text{As})_z\text{-nSi}_{1-x}\text{Ge}_x\text{-n(Si}_{1-x}\text{Ge}_x)_{1-z}(\text{Al}_{1-y}\text{Ga}_y\text{As})_z$ are obtained, with a surface layer that can be described as $\text{Al}_{0.08}\text{Ga}_{0.06}\text{As}_{0.14}$. The study of some electrophysical and photoelectric properties of the films showed that these films and structures have a specific character. The above features of the technological process of obtaining these epitaxial layers and structures based on them in the future will make it possible to use the obtained heterostructures in the production of optoelectronic devices.

References

- [1] A. Mukherjee, D. Ren, P.E. Vullum, J. Huh, B.O. Fimland, H. Weman, *ACS Photonics* **8**, 2355 (2021).
- [2] L.S. Lunin, M.L. Lunina, O.V. Devitsky, I.A. Sysoe, *Semiconductors* **51**, 387 (2017).
- [3] E. Hughes, R. D. Shah, K. Mukherjee, *J. Appl. Phys.* **125**, 16 (2019).
- [4] N. Jain, M.K. Hudait, *Energy Harvest. Syst.* **121**, 1 (2014).
- [5] A. Onno, M. Tang, M. Wang et al., in: *IEEE 44th Photovoltaic Specialist Conference (PVSC), Washington (DC)*, 2017.
- [6] J.P. van der Ziel, R.A. Logan, N. Chand, *J. Appl. Phys.* **64**, 3201 (1988).
- [7] X. Zhao, K.H. Montgomery, J.M. Woodall, in: *IEEE 40th Photovoltaic Specialist Conference (PVSC), Denver (CO)*, 2014.
- [8] G. Boras, X. Yu, H.A. Fonseca et al., *J. Phys. Chem. C* **125**, 26 (2021).
- [9] R. Venkatasubramanian, M. Timmons, *Solid-State Electron.* **37**, 1809 (1994).
- [10] N. Baidus, V. Aleshkin, A. Dubinov et al., *Crystals* **8**, 311 (2018).
- [11] S.A. Ringel, J.A. Carlin, C.L. Andre et al., *Prog. Photovolt. Res. Appl.* **417**, 10 (2002).
- [12] W.-C. Kuo, H-C. Hsieh, W. Chih-Hung, H. Wen-Hsiang, C.-C. Lee, J.-Y. Chang *Int. J. Photoenergy* **2016**, 7218310 (2016).
- [13] G.B. Stringfellow, P.E. Green, *J. Electrochem. Soc.* **117**, 1075 (1970).
- [14] M. Rubinstein, *J. Electrochem. Soc.* **752**, 113 (1966).
- [15] A.J. McAlister, D.J. Kahan, *Bull. Alloy Phase Diagrams* **410**, 4 (1983).